Analyzing Free Vibration of a Cantilever Microbeam Submerged in Fluid with Free Boundary Approach

K. Ivaz[1][†], D. Abdollahi[1] and R. Shabani[2]

[1] *University of Tabriz, Tabriz, East Azarbayjan, Iran*
[2] *Urmia University, Urmia, West Azarbayjan, Iran*

†*Corresponding Author Email: ivaz@tabrizu.ac.ir*

ABSTRACT

This paper aims to present a detailed analysis of the free vibration of a cantilever microbeam submerged in an incompressible and frictionless fluid cavity with free boundary condition approach. In other words, in addition to the kinematic compatibility on the boundary between microbeam and its surrounding fluid, equations of the potential functions are modeled assuming the free boundaries. Galerkin's method is used for simulations. The results of the proposed model are validated by comparing with the early analytical and numerical studies of pertinent literature. Finally, it is inferred that by involving the free boundary conditions, which is closer to the physical reality, the natural frequencies of the system have instability, especially in higher modes. In addition, the values obtained for natural frequencies are smaller than what were calculated by fixed bounary approach.

Keywords: Vibration; Free boundary equation; Added mass; Microbeam.

1. INTRODUCTION

The theory of beams have been studied over the years by many scientists in various majors. Microbeams with different end conditions are used in many micro-devices such as biology, geology, micro-resonators, nuclear science, and micro-actuators, Hung (1999). Fluid-structure interaction problems have been considered since 1963 (Eisley (1964), Leissa (1969), Liang (2012)). Lindholm *et al*. (1965) examined the vibration of cantilever plates in air and water in 1965. They compared their results with theoretical predictions using simple beam theory and thin-plate theory. Atkinson and Manrique de Lara (2007) provided a method to calculate the frequency response of a rectangular cantilever plate vibrating in a viscous fluid. Their work dealt with obtaining an expression related to the pressure of the surrounding fluid on the plate. This expression constituted the fluid reaction needed to solve the balance of forces on the plate. Esmailzadeh *et al*. (2008) studied numerically the dynamic behavior of a 3D thin flexible structure in invisid incompressible stationary fluid using a combination of classical thin plate theory and finite element analysis. Rezazadeh *et al*. (2009) investigated the effects of surrounding fluid on the mechanical behavior of electrostatically actuated cantilever micorbeams. They considered that increasing the aspect ratio of the beam of increasing the fluid density increases the added mass and

decreases the natural frequency of the beam.

Akgoz and Civalek (2014) studied thermo-mechanical buckling behavior of functionally graded microbeams embedded in elastic medium based on trigonometric shear deformation beam and modified coupled stress theories. They determined effects of thickness to material length scale parameter ratio, material property gradient index, length to thickness ratio and temperature change. Wang *et al*. (2015) introduced a mathematical model and a numerical algorithm for the bending and post-buckling of a microbeam within the context of Euler- Bernoulli beam theory involving geometric nonlinearity.

Park and Kim (2005) studied the existence of the solution to the mixed problem for Euler-Bernoulli beam equation with memory condition at the boundary. They proved that the energy decay with the same rate of decay of the relaxation function. In this paper, we present a detailed analysis of the frequency response of a cantilever beam submerged in fluid and excited by an arbitrary driving force with free boundary approach. It is important to mention that we do not neglect the free boundary effects. The dynamic response of an electrostatically actuated micro-beam immersed in an incompressible viscous fluid cavity was analyzed with free boundary approach by Abdollahi *et al.* (2016a).

The approach of this study is based on both finite

difference and finite element methods for the solution of cantilever microbeam. An imaginary fluid-fluid interface with equal kinematic conditions around the beam-fluid interface is considered for the analysis of the derived eigenvalue problem. Galerkin's method is applied for the simulation of the proposed system, because of its ability to deal with complex 2D and 3D domains with ease. Moreover, we would be able to overcome the nonlinearity of the boundary conditions in free boundary approach by this method. Furthermore, we have used the free vibration modes of beam in air as basis in our simulation.

In Section 2, the governing equations are derived from applying linear superposed mode shapes. Section 3 verifies the model for various aspect and thickness ratios. In Section 4, an example is investigated by free boundary conditions. Finally, Section 5 completes this study with a brief conclusion.

2. MATHEMATICAL MODEL

The free vibration and natural frequencies of a cantilever microbeam submerged in a bounded incompressible and inviscid fluid domain was analyzed by Shabani *et al.* (2013) regarding fixed boundary. We sketched the following model for the same system with free boundary approach considering that the beam-fluid interface has not fixed hight throughout the length of the microbeam along the x coordinate (see Abdollahi *et al.* (2016b) for more details). Fig. 1 shows a cantilever microbeam with the length l submerged in a cavity with the width a longer than l making it possible for two fluid domains to interact. The off-center position of the beam is specified by its distance from the lower and upper sides of the cavity, H_1 and H_2, respectively. The width of the microbeam and cavity are assumed equal to b. It should be noted that the fluid is assumed incompressible and the amplitude of vibration must be small.
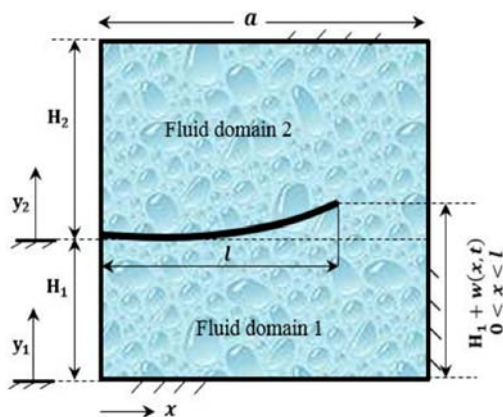
Fig. 1. Cantilever microbeam submerged in a fully contained cavity.

The governing equations of the system were written as follows:

$$EI \frac{\partial^2 w}{\partial x^4} + \rho_B \frac{\partial^2 w}{\partial t^2} = b(P_1 - P_2), 0 < x < l, t > 0 \quad (1)$$

where EI is the bending stiffness of the microbeam, ρ_B is the mass per unit length and $w(x,t)$ describes the deflection at point x along the length of the microbeam with the following set of boundary and initial conditions:

$$
\begin{cases}
w\big|_{x=0} = 0, t > 0 \\
\dfrac{\partial^2 w}{\partial x^2}\Big|_{x=l} = 0, \dfrac{\partial^3 w}{\partial x^3}\Big|_{x=l} = 0, t > 0 \\
w\big|_{t=0} = f(x), \dfrac{\partial w}{\partial t}\Big|_{t=0} = g(x), 0 < x > l
\end{cases}
$$
(2)

in which $f(x)$ and $g(x)$ are the values of transverse displacement and velocity, respectively. P_1 and P_2 are the fluid pressures in the cavity with the relations (Shababi (2013)) as follows:

$$
\begin{cases}
P_1 = -\rho_f \dfrac{\partial \varphi_1(x, y_1, t)}{\partial t}\Big|_{y_1 = H_1 + w(x,t)}, (a) \\
P_2 = -\rho_f \dfrac{\partial \varphi_2(x, y_2, t)}{\partial t}\Big|_{y_2 = w(x,t)}, (b)
\end{cases}
\quad (3)
$$

where φ_1 and φ_2 are the velocity potential of the fluids of the microbeam in the lower and upper regions with the density ρ_f which should be satisfied in the following Laplace equations with free boundary domains:

$$
\nabla^2 \varphi_1(x, y_1, t) = 0,
$$
$$
\begin{cases}
0 < x < l, 0 < y_1 < H_1 + w(x,t) \\
l < x < a, 0 < y_1 < H_1
\end{cases}
\quad (4)
$$

$$
\nabla^2 \varphi_2(x, y_2, t) = 0,
$$
$$
\begin{cases}
0 < x < l, w(x,t) < y_2 < H_2 \\
l < x < a, 0 < y_2 < H_2
\end{cases}
\quad (5)
$$

which the boundary conditions reads as follows:

$$
\begin{cases}
\frac{\partial \varphi_1}{\partial x}\big|_{x=0,a} = 0 & 0 < y_1 < H_1, \ (a) \\
\frac{\partial \varphi_1}{\partial y_1}\big|_{y_1=0} = 0 & 0 < x < a, \ (b) \\
\begin{cases}
\frac{\partial \varphi_1}{\partial n_Q}\big|_{y_1=H_1+w} = \frac{\partial w}{\partial t}, & 0 < x < l \ (c) \\
\frac{\partial \varphi_1}{\partial y_1}\big|_{y_1=H_1} = \frac{\partial \varphi_2}{\partial y_2}\big|_{y_2=0}, & l < x < a \ (d)
\end{cases}
\end{cases}
$$
(6)

$$
\begin{cases}
\frac{\partial \varphi_2}{\partial x}\big|_{x=0,a} = 0 & 0 < y_2 < H_2, \ (a) \\
\frac{\partial \varphi_2}{\partial y_2}\big|_{y_2=H_2} = 0 & 0 < x < a, \ (b) \\
\begin{cases}
\frac{\partial \varphi_2}{\partial n_Q}\big|_{y_2=w} = \frac{\partial w}{\partial t}, & 0 < x < l \ (c) \\
\frac{\partial \varphi_2}{\partial y_2}\big|_{y_2=0} = \frac{\partial \varphi_1}{\partial y_1}\big|_{y_1=H_1}, & l < x < a \ (d)
\end{cases}
\end{cases}
$$
(7)

in which $\dfrac{\partial \varphi}{\partial n_Q}$ is the directional derivative of φ in the direction of the unit vector n_Q. Eqs. (6a) and (6b) mean that there is no fluid velocity close to the walls of the cavity in the directions of both x and y axes. These boundary conditions are the same for the velocity of fluid in the upper domain of the cavity, as well. Moreover, Eqs. (6c) and (7c) show that the velocities of the fluid is equal to of the microbeam throughout the length of the beam in the common boundary. Likewise, Eqs.(6d) and (7d) state that the fluids of upper and lower domains have the same velocity at the height $y_1 = H_1$ via $l < x < a$.

A system of boundary integral equations was established to solve the Eqs. (1-7) in Abdollahi *et al.* (2016b). The existence and uniqueness of the solution were proved by the use of Banach fixed point theorem. As a result, the natural frequencies were affected in comparison with pertinent literature Liang (2012), Lindholm (1965) and Shabani (2013). The aim of this paper is to investigate the problem with free boundary approach. The method of separation of variables is applied to solve Eqs. (4) and (5) by imposing the fixed boundary conditions (6a, 6b) and (7a, 7b). Therefore, the following relations are obtained for the velocity potential functions $\varphi_1(x, y_1, t)$ and $\varphi_2(x, y_2, t)$ as follows:

$$\begin{cases} \varphi_1 = \sum_{i=1}^{\infty} A_{i(t)} \cos(\lambda_i x) \cosh(\lambda_i y_1), & (a) \\ \varphi_2 = \sum_{i=1}^{\infty} E_i(t) \cos(\lambda_i x) \begin{bmatrix} \cosh(\lambda_i y_2) \\ -\tanh(\lambda_i H_2) \sinh(\lambda_i y_2) \end{bmatrix}, & (b) \end{cases}$$
(8)

where the eigenvalues λ_i is equal to $i\pi/a$, and $A_i(t)$ and $E_i(t)$ are unknown modal amplitudes of fluid oscillation. The lateral motion of the microbeam, $w(x,t)$ is formulated as a linear superposition of the free vibration modes in air as follows:

$$w(x,t) = \sum_{i=1}^{\infty} q_i(t) \psi_i(x),$$
(9)

in which $\Psi_i(x)$ is the natural mode shapes of the microbeam in air and the unknown generalized coordinates $q_i(t)$ should be estimated. The mode shapes are written as (Abdollahi *et al.* (2013)):

$$\psi_i = (\sinh(\beta_i l) + \sin(\beta_i l)) \times (\cosh(\beta_i x) - \cos(\beta_i x))$$
$$-(\cosh(\beta_i l) + \cos(\beta_i l)) \times (\sinh(\beta_i x) - \sin(\beta_i x))$$
(10)

where values of $\beta_i l$ must satisfy the transcendental equation

$$\cosh(\beta_i l) \cos(\beta_i l) = -1.$$
(11)

For $i = 1,2$ the solutions are $\beta_1 l \simeq 1.875104$, , $\beta_2 l \simeq 4.694091$ and as $i \to \infty$, the values of βil approaches to the value $\left(i - \dfrac{1}{2}\right)\pi$. It should be mentioned that the values $\beta_i l$ and the natural frequencies of the dry beam (ωi) is satisfied in Abdollahi *et al.* (2016b)

$$\omega_i = (\lambda_i l)^2 \sqrt{\dfrac{EI}{\rho_B l^4}}.$$
(12)

By substituting Eqs. (8) and (9) into the kinematic beam-fluid conditions (6c and d) and (7c and d) yields the following relations:

$$\sum_{i=1}^{\infty} A_i(t)\lambda_i \cos(\lambda_i x) \sinh\left[\lambda_i(H_1 + w(x,t))\right] \times \dfrac{1}{\sqrt{1 + w_x^2(x,t)}}$$
$$-\sum_{i=1}^{\infty} A_i(t)\lambda_i \sin(\lambda_i x) \times \cosh\left[\lambda_i(H_1 + w)\right] \dfrac{w_x(x,t)}{\sqrt{1 + w_x^2}} =$$
$$\begin{cases} \sum_{i=l}^{\infty} q_i(t)\psi_i(x), \\ \sum_{i=1}^{\infty} E_i(t)\lambda_i \cos(\lambda_i x)\left[-\tanh(\lambda_i H_2)\right], \end{cases}$$
(13)

$$\sum_{i=1}^{\infty} E_i(t)\lambda_i \cos(\lambda_i x)$$
$$\left[\sinh(\lambda_i w(x,t)) - \tanh(\lambda_i H_2) \times \cosh(\lambda_i w(x,t))\right]$$
$$\dfrac{1}{\sqrt{1 + w_x^2}} - \sum_{i=1}^{\infty} E_i(t)\lambda_i \sin(\lambda_i x)$$
$$\times \left[\cosh(\lambda_i w(x,t)) - \tanh(\lambda_i H_2)\sinh(\lambda_i w(x,t))\right]$$
$$\times \dfrac{w_x}{\sqrt{1 + w_x^2}} = \begin{cases} \sum_{i=l}^{\infty} q_i(t)\psi_i(x), \\ \sum_{i=1}^{\infty} A_i(t)\lambda_i \cos(\lambda_i x)\sinh(\lambda_i H_1), \end{cases}$$
(14)

Both sides of the Eqs. (13) and (14) are multiplied by $\cos(\lambda_i x)$ and then integrated over $0 < x < a$ to obtain the following relations:

$$\sum_{i=1}^{\infty} A_i(t)\lambda_i \left[\wedge_1(t) + \wedge_2(t)\right]_{ji} =$$
$$\sum_{i=1}^{\infty} q_i(t)\alpha_{ji} - \sum_{i=1}^{\infty} E_i(t)\lambda_i \mu_{ji} \tanh(\lambda_i H_2),$$
(15)

$$\sum_{i=1}^{\infty} E_i(t)\lambda_i \left[\wedge_3(t) + \wedge_4(t)\right]_{ji} =$$
$$\sum_{i=1}^{\infty} q_i(t)\alpha_{ji} + \sum_{i=1}^{\infty} A_i(t)\lambda_i \mu_{ji} \sinh(\lambda_i H_1),$$
(16)

where coefficients μ_{ji}, α_{ji} αji and $\Lambda_i(t)(1 \le i \le 4)$ are defined as:

$$\begin{cases} \alpha_{ji} = \int_0^l \cos(\lambda_j x)\psi_i(x)\,\mathrm{d}x, \\ \mu_{ji} = \int_0^l \cos(\lambda_i x)\cos(\lambda_j x)\,\mathrm{d}x, \\ \Lambda_1(t) = \int_0^a \frac{\cos(\lambda_i x)\sinh[\lambda_i(H_1+w)]}{\sqrt{1+w_x^2}}\cos(\lambda_j x)\,\mathrm{d}x, \\ \Lambda_2(t) = \int_0^a \frac{\sin(\lambda_i x)\cosh[\lambda_i(H_1+w)]w_x}{\sqrt{1+w_x^2}}\cos(\lambda_j x)\,\mathrm{d}x, \\ \Lambda_3(t) = \int_0^a \cos(\lambda_i x)\Big[\sinh(\lambda_i w) \\ \qquad -\tanh(\lambda_i H_2)\cosh(\lambda_i w)\Big]\frac{\cos(\lambda_j x)}{\sqrt{1+w_x^2}}\,\mathrm{d}x, \\ \Lambda_4(t) = \int_0^a \sin(\lambda_i x)\Big[\cosh(\lambda_i w) \\ \qquad -\tanh(\lambda_i H_2)\sinh(\lambda_i w)\Big]\frac{w_x}{\sqrt{1+w_x^2}}\cos(\lambda_j x)\,\mathrm{d}x. \end{cases} \tag{17}$$

Substituting Eqs. (8) into Eq. (3) and inserting the outcome into Eq. (1), the equation of motion for the microbeam yields the following form:

$$EI\sum_{i=1}^{\infty}q_i(t)\psi_i^{IV}(x)+\rho_B\sum_{i=1}^{\infty}q_i(t)\psi_i(x) =$$

$$-b\rho_f\begin{bmatrix} \sum_{i=1}^{\infty}\dot{A}_i(t)\cos(\lambda_i x)\cosh[\lambda_i(H_1+w)] \\ -\sum_{i=1}^{\infty}\dot{E}_i(i)\cos(\lambda_i x)\begin{pmatrix}\cosh[\lambda_i w(x,t)]\\-\tanh(\lambda_i H_2)\sinh[\lambda_i w(x,t)]\end{pmatrix} \end{bmatrix} \tag{18}$$

Making use of the orthogonality of beam mode shapes over $0 \leq x \leq l$, the following equation is derived:

$$\left[EI\int_0^l\psi_i^{IV}(x)\psi_i(x)dx\right]q_j(t)$$

$$+\left[\rho_B\int_0^l\psi_i^2(x)dx\right]\times\ddot{q}_i(t)=$$

$$-b\rho_f\left[\sum_{i=1}^{\infty}\dot{A}_i(t)\int_0^l\cos(\lambda_i x)\times\right.$$

$$\cosh[\lambda_i(H_1+w)]\psi_j(x)dx$$

$$\left.-\sum_{i=1}^{\infty}\dot{E}_i(t)\times\int_0^l\cos(\lambda_i x)\begin{pmatrix}\cosh[\lambda_i w(x,t)]\\-\tanh(\lambda_i H_2)\\\times\sinh[\lambda_i w(x,t)]\end{pmatrix}\psi_j(x)dx\right] \tag{19}$$

Now, the microbeam and fluid vibration modes are truncated to n and m modes, respectively. Therefore, the finite set of matrix equations is derived by rewriting Eqs. (15), (16) and (19) as follows:

$$[L]\{A\}=[D]\{\dot{q}\}-[G]\{E\}, \tag{20}$$

$$-[R]\{E\}=[D]\{\dot{q}\}+[K]\{A\}, \tag{21}$$

$$[F]\{q\}+[M]\{\ddot{q}\}=-[C]\{\dot{A}\}-[J]\{\dot{E}\}, \tag{22}$$

where the elements of the coefficient matrices are

calculated by the following relations:

$$\begin{cases} L_{ij}=\lambda_j[\Lambda_1(t)+\Lambda_2(t)]_{ij}, \\ D_{ij}=\alpha_{ij}, \\ G_{ij}=\lambda_j\mu_{ij}tanh(\lambda_j H_2), \\ R_{ij}=\lambda_j[\Lambda_3(t)+\Lambda_4(t)]_{ij}, \\ K_{ij}=\lambda_j\mu_{ij}\sinh(\lambda_j H_1), \\ F_{ii}=EI\int_0^l\psi_i^{IV}(x)\psi_i(x)\,\mathrm{d}x, \\ M_{ii}=\rho_B\int_0^l\psi_i^2(x)\,\mathrm{d}x, \\ C_{ij}=b\rho_f\int_0^l\cos(\lambda_j x) \\ \qquad\times\cosh[\lambda_j(H_1+w(x,t))]\psi_i(x)\,\mathrm{d}x, \\ J_{ij}=-b\rho_f\int_0^l\cos(\lambda_j x)\Big(\cosh[\lambda_j w] \\ \qquad-\tanh(\lambda_j H_2)\sinh[\lambda_j w]\Big)\psi_i(x)\,\mathrm{d}x. \end{cases} \tag{23}$$

By considering the time step size $\delta t > 0$, the solution would be estimated at times $t^i = i\,\delta t$. First, the generalized fluid coordinates A and E are calculated from Eqs. (20) and (21). Then, the outcomes are substituted into Eq. (22) by using the notation $q^i = q\left(t^i\right)$ and forward difference approximation. Therefore, the following linear algebraic system with n unknowns and equations is obtained as an iterative scheme:

$$([M^i]+[C^iM_1^{i+1}])+[J^iM_2^{i+1}])\{q^{i+2}\}=([2M^i]$$

$$+[C^i(M_1^{i+1}+M_1^i)]+[J^i(M_2^{i+1}+M_2^i)])\{q^{i+1}\}$$

$$-([M^i]+(\delta t)^2[F^i]+[C^iM_1^i]+[J^iM_2^i])\{q^i\}, \tag{24}$$

where M_1 and M_2 are defined as follows:

$$\begin{cases} M_1=[L^{-1}D]-[L^{-1}G]([KL^{-1}G]-[R])^{-1} \\ \qquad([D]+[KL^{-1}D]), \\ M_2=([KL^{-1}G]-[R])^{-1}([D]+[KL^{-1}D]). \end{cases} \tag{25}$$

and the superscripts of the coefficient matrices have been introduced for the time index.

The terms $\left[C^iM_1^{i+1}\right]$ and $\left[J^iM_2^{i+1}\right]$ [JiMi2+1] in Eq. (24) are the added mass matrices of the fluid domains 1 and 2, respectively. These two-part added mass are the result of the presence of the fluid around the microbeam.

The right-hand side of Eq. (24) is known, but the left-hand side involves n unknown generalized coordinates $\{q\}$. Using Eq. (9) in the first initial condition of Eq. (2), we get

$$q_j^0=\frac{1}{\int_0^l\psi_j^2(x)dx}\int_0^l f(x)\psi_j(x)dx, \tag{26}$$

for $j = 1,2,...,n$ and the second initial condition (2c) can be approximated as

Table 1 Comparison of(fundamental) frequencies in air ω1 (Hz)

Aspect ratio, L/b	5	3	2	1
Thickness ratio, h/b	0.124	0.061	0.061	0.024
Analytical (Liang et al. (2012))	20.57	28.37	64.29	101.2
Experimental (Lindholm et al. (1965))	19.4	27.3	60.7	96.3
Fixed boundary (Shabani et al. (2013))	20.51	28.07	63.15	98.4
Proposed method	20.49	27.98	63.12	98.54

Table 2 Comparison of (fundamental) frequencies in water ω1 (Hz)

Aspect ratio, L/b	5	3	2	1
Thickness ratio, h/b	0.124	0.061	0.061	0.024
Analytical (Liang et al. (2012))	15.63	18.30	42.30	51.93
Experimental (Lindholm et al. (1965))	14.60	17.80	40.30	51.40
Fixed boundary (Shabani et al. (2013))	15.62	18.82	46.80	57.90
Analytical (Abdollahi et al. (2016))	13.09	17.89	40.24	59.33
Proposed method	14.93	18.12	43.62	54.38

Table 3 The data used in the calculations

Parameters	Value
Microbeam width, b	50 μm
Microbeam length, l	250 μm
Microbeam thickness, h	3 μm
Container length, a	350 μm
Liquid depth of domain 1, H_1	200 μm
Liquid depth of domain 2, H_2	300 μm
Container height, H	500 μm
Young's modulus, E	169 Gpa
Fluid density, ρ_f	1000 kg/m^3
Microbeam mass, ρ_B	3.4965×10^{-7} kg/m
Poisson's ratio, υ	0.06

$$q_j^1 = q_j^0 + \frac{1}{\int_0^l \psi_j^2(x)dx} \int_0^l \delta t g(x)\psi_j(x)dx. \qquad (27)$$

for $j = 1,2,...,n$. Therefore, Eq. (24), using Eqs. (26) and (27) as initial guesses can be solved to find q^{i+2} in any step $i = 0,1,...$. So, the unknown functions $w(x,i\delta t)$ can be found in any time $t = i\delta t, i$

$= 1,2,....$ For this aim, the intervals [0,*l*] and [l,a] are divided to 70 and 30 nodes throughout x direction in the cavity, respectively. Moreover, seven fluid oscillation modes ($m = 7$) in Eq. (8) and five modes (n = 5) in Eq. (9) are selected to get the results.

3. VERIFICATION OF THE METHOD

Tables 1 and 2 present the comparison of

fundamental frequencies in air $\left(\rho = 1.3 \ {}^{kg}\!\!\diagup\!\!_{m^3} \right)$ and water $\left(\rho_f = 1000 \ {}^{kg}\!\!\diagup\!\!_{m^3} \right)$ with the experimental results of Lindholm *et al.* (1965), and the analytical results of Liang *et al.* (2012), Shabani *et al.* (2013) and our recent work in Ref. Abdollahi *et al.* (2016b). These results validates the proposed method with free boundary approach for various aspect and thickness ratios.

4. AN EXAMPLE

In this section, an illustrated example is presented to compare the natural frequencies and mode shapes of the microbeam submerged in water with both fixed and free boundary approach. The material properties and the values of the used constants are listed in Table 3. The values of transverse displacement $f(x)$ and the velocity $g(x)$ in Eq.(2) are assumed as $-0.05x$ and zero, respectively. The width of the microbeam meets $b \geq 5h$. Consequently, the microbeam strain conditions should be taken into consideration. Therefore, E is replaced by $E/\left(1 - \upsilon^2\right)$, where υ is Poisson's ratio. Fig. 2 shows the mode shapes of the microbeam with both fixed and free boundary approach. It is shown that the deviation increases for higher modes. The fluid movement patterns in Figs. 3 and 4 confirm the mode shapes presented in Fig. 2 as it was expected. The fluid movement intense for higher modes around the microbeam. Fig. 5 presents the natural frequencies of the microbeam with fixed and free boundary states. It is inferred that the free boundary conditions in the velocity potential functions affect the consecutive modes of the microbeam. Therefore, the oscillatory property of $w(x,t)$ has been transmitted on the natural frequencies of the microbeam. It means that by assuming free bouandary conditions in the equations of the potential functions, which is closer to the physical reality, the natural frequencies of the system are not fixed. Fig. 6 depicts that as the number of fluid modes increases, the rate of convergence grows reasonably. Fig. 7 suggests the natural frequencies of the wet microbeam as a function of its off-center position $H_1/\left(H_1 + H_2\right)$. The graphs depict that the natural frequencies decrease when the micobeam is close to the top or bottom surfaces. Nevertheless, the frequencies are not affected much for different off-center location of the microbeam. Fig. 8 proves that increasing the length of the microbeam decreases the natural frequencies and changes the fluid moving patterns in the two proposed approach. It is well known that the natural frequencies of a beam is strongly dependent on the fluid in which it is submerged. Fig. 9 investigates the sensitivity of the system to the fluid density. It illustrates that the sensitivity of frequencies decreases for the higher densities. Fig. 11-13 depict the values of velocity and pressure of fluid inside the cavity.
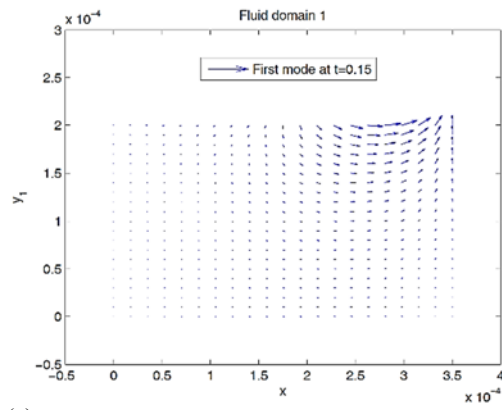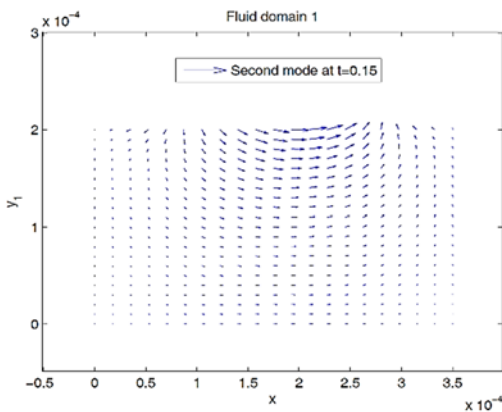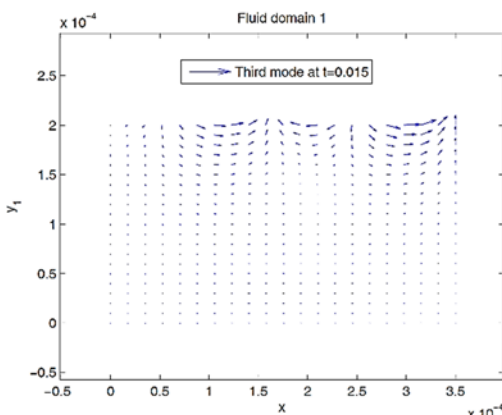

(a)　　　　First mode

(b)　　　　Second mode

(c)　　　　Third mode

(d)　　　　Fourth mode
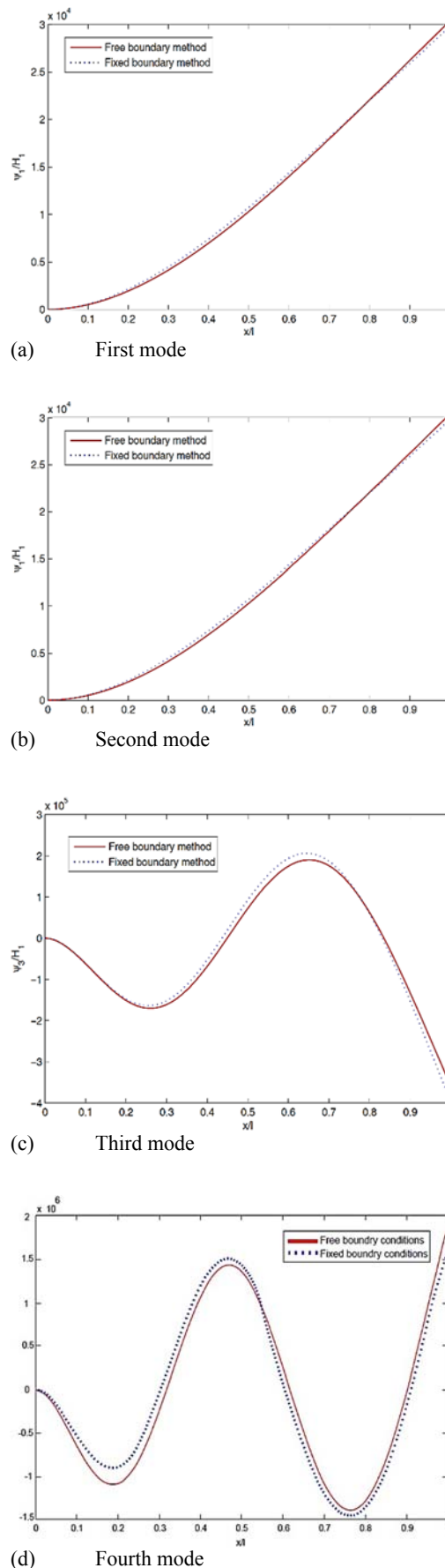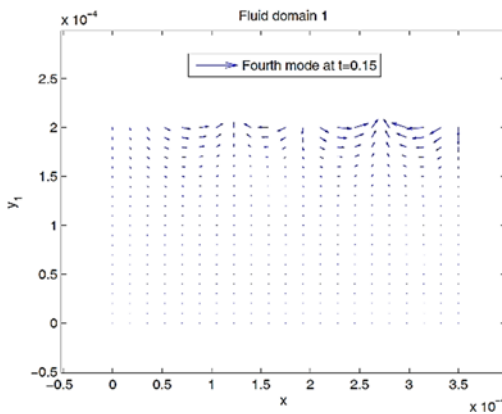
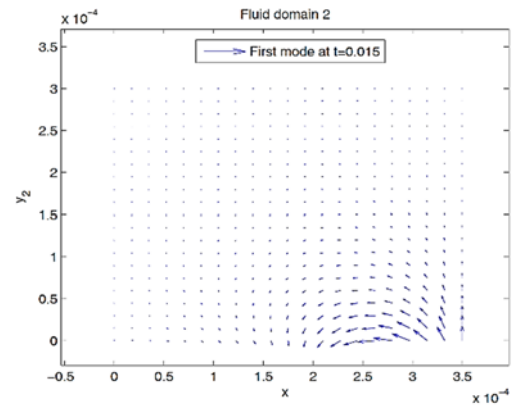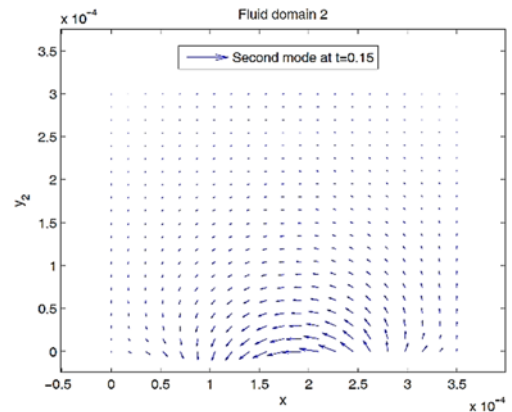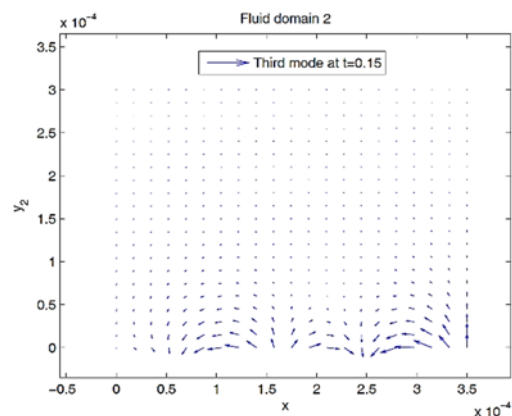**Fig. 2. The deviation of the mode shapes of the wet microbeam.**

(a)

(b)

(c)

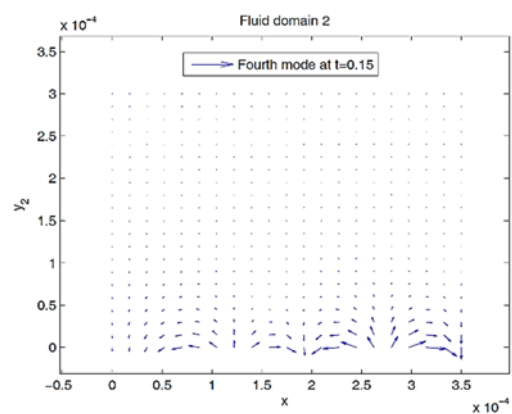(d)

Fig. 3. The fluid movement patterns in domain 1.

(a)

(b)

(c)

(d)

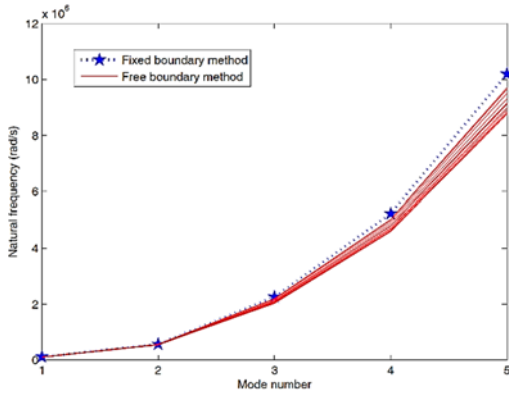Fig. 4. The fluid movement patterns in domain 2.

Fig. 5. Variations of the natural frequencies of the wet microbeam with fixed and free boundary approach.
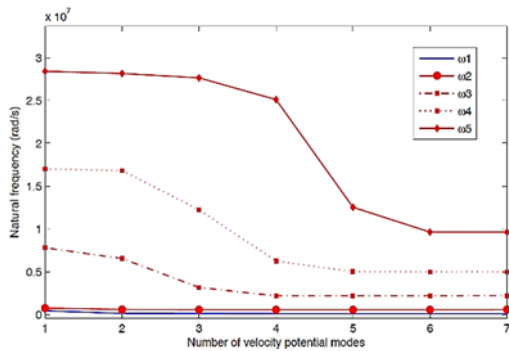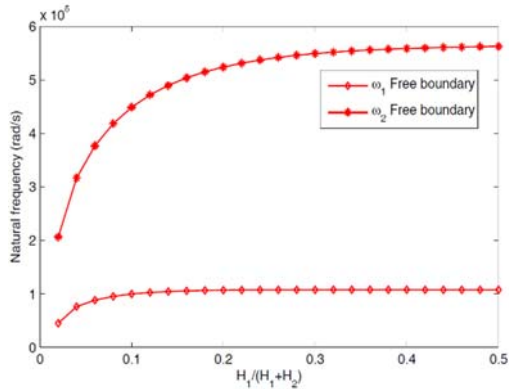

Fig. 8. Variations of the natural frequencies of the wet microbeam with free boundary conditions.

Fig. 6. Convergency of the natural frequencies of the wet microbeam by free boundary condition.

(a)
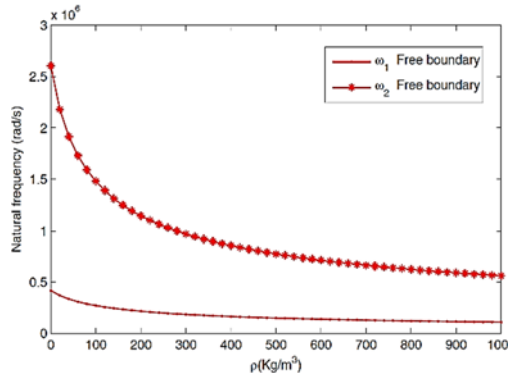
(a)
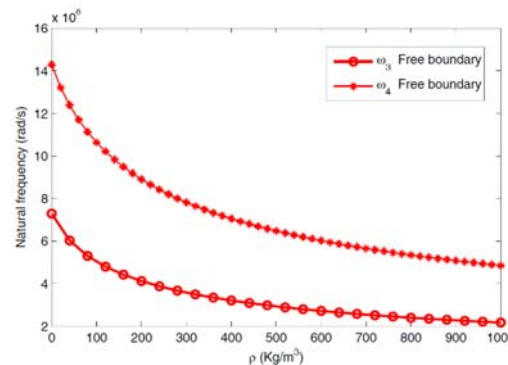
(b)

Fig. 9. Natural frequencies as a function of fluid density with free boundary conditions.
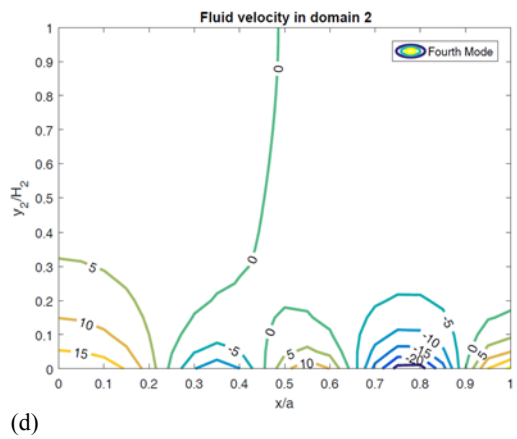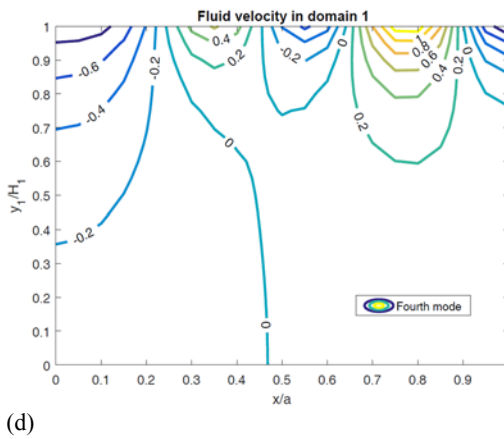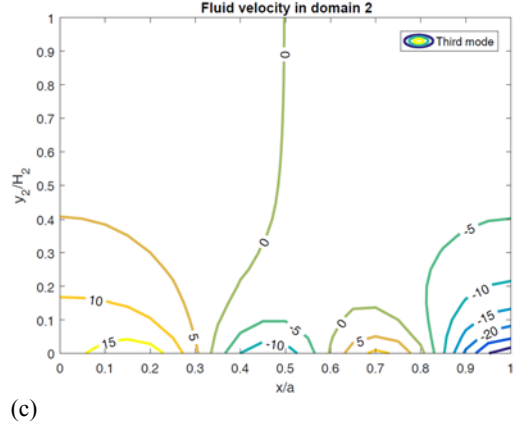

(b)

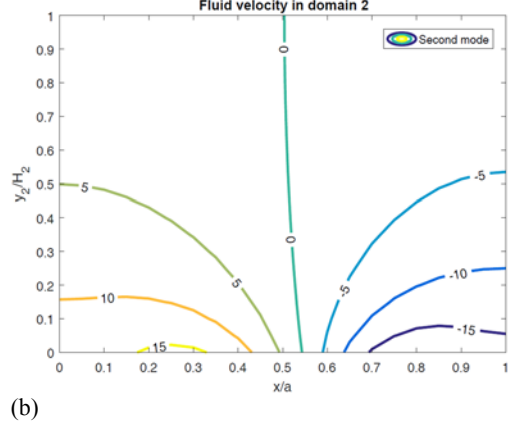**Fig. 7. The comparison of the effects of vertical position on natural frequencies in fixed and free bounday states.**
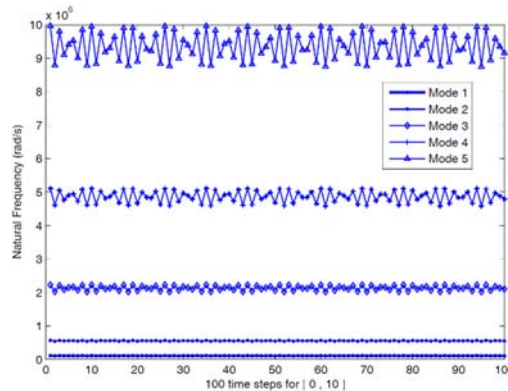
Fig. 10. The comparison of the four natural frequencies of the beam with free boundary conditions.

(a)

(a)

(b)

(b)

(c)

(c)

(d)
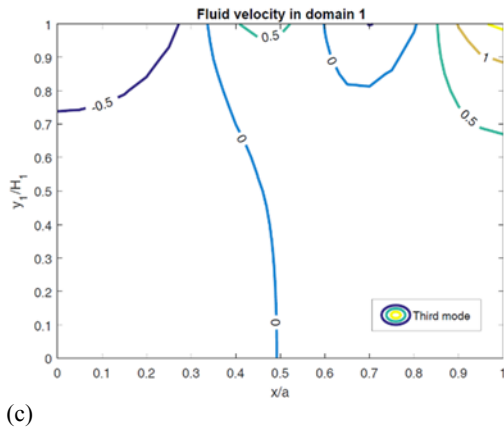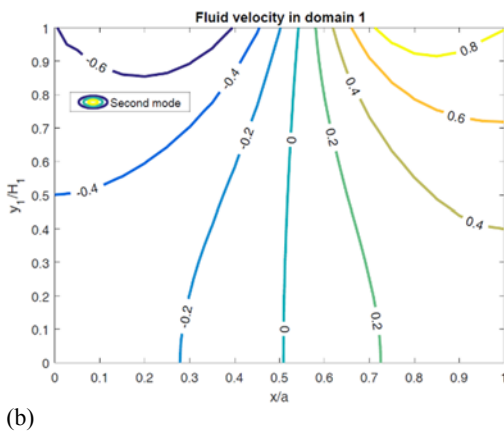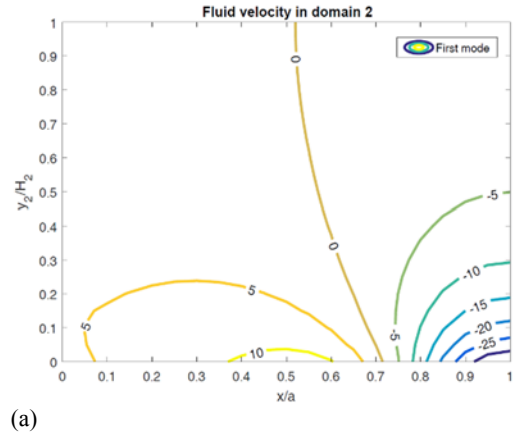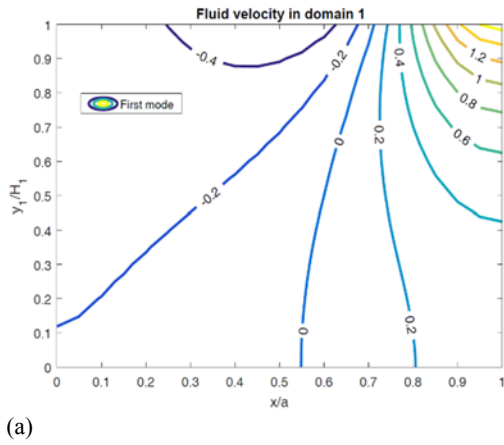
Fig. 11. The fluid velocities patterns in domain 1.

(d)

Fig. 12. The fluid velocities patterns in domain 2.
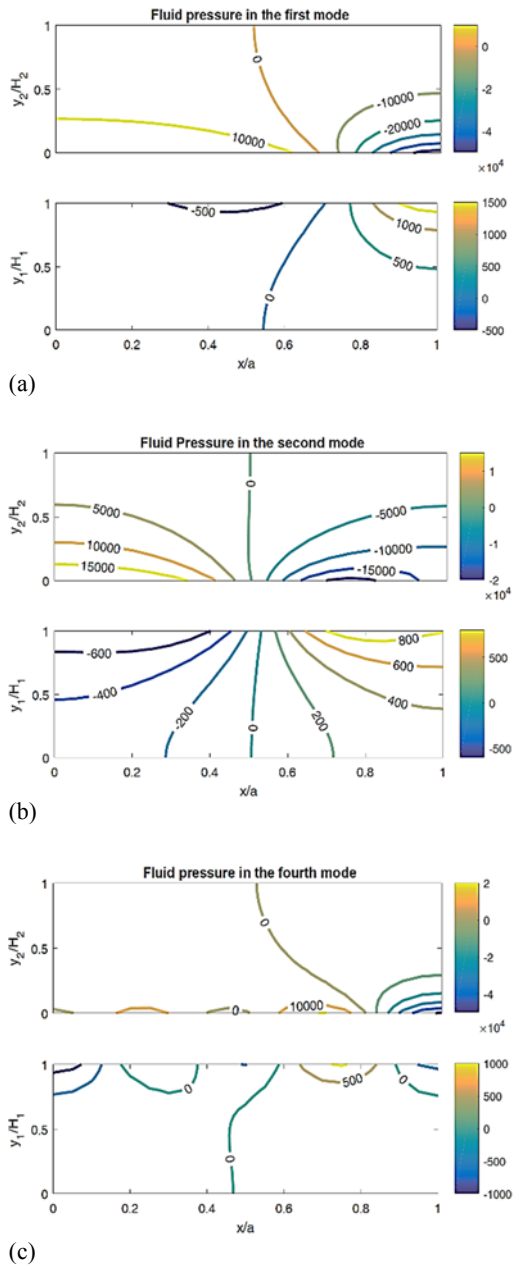
(a)

(b)

(c)

Fig. 13. The fluid pressure patterns.

5. CONCLUSIONS

This paper investigates the effect of fluid-structure interaction on the free vibration of a microbeam submerged in an incompressible fluid with free boundary condition approach. The potential equations governing on the fluid have been modeled considering the free boundary conditions which is closer to the physical reality. Galerkin's semi-analytical method was utilized to solve the coupled equations. Fig. 10 reveals that the natural frequencies of the microbeam are influenced by the presence of $w(x,t)$ in the domains of the velocity potential functions φ_1 and φ_2 in Eqs. (4) and (5). It shows that the consecutive natural frequencies of the system have oscillations and this instability increases for higher modes, whereas, the all similar results by

fixed boundary conditions were fixed and greater in pertinent literature. Consequently, it is inferred that in addition to the conditions of kinematic compatibility of the fluid-structure, involving of free boundary condition in the proposed model affects the natural frequencies, especially in higher modes.

REFERENCES

Abdollahi, D., K. Ivaz and R. Shabani (2016b). A numerical improvement in analyzing the dynamic characteristics of an electrostatically actuated micro-beam in fluid loading with free boundary approach. International *Journal of Engineering-Transactions A: Basics 29*(7), 1005-1013.

Abdollahi, D., S. Ahdiaghdam, K. Ivaz and R. Shabani (2016a). A theoretical study for the vibration of a cantilever microbeam as a free boundary. *Applied Mathematical Modelling 40*, 1836-1849.

Akgoz, B. and O. Civalek (2014). Thermo mechanical buckling behavior of functionally graded microbeams embedded in elastic medium. *International Journal of Engineering Science 85*, 90-104.

Atkinson, C. and M. Manrique Lara (2007). The frequency response of a rectangular cantilever plate vibrating in a viscous fluid. *Journal of Sound and Vibration 300*, 352-367.

Eisley, J. G. (1964). Nonlinear vibration of beams and rectangular plates. Journal of Applied Mathematics and Physics 15.2, 167-175.

Esmailzadeh, M., A. A. Lakis, M. Thomas and L. Marcouiller (2008). Three-dimensional modeling of curved structures containing and/or submerged in fluid. *Finite Elements in Analysis and Design 44*, 334 - 345.

Hung, E. S. and S. D. Senturia (1999). Extending the travel range of analogtuned electrostatic actuators. *Journal of Microelectromechanical Systems 8*, 497-505.

Leissa, A. W. (1969). *Vibration of plates*. Ohio State Univ. Columbus.

Liang Ke, L., Y. S. Wang and J. Yang (2012). Nonlinear free vibration of size-dependent functionally graded microbeams. *International Journal of Engineering Science 50*(1), 256-267.

Lindholm, U. S., D. D. Kana, W. H. Chu and H. N. Abramson (1965). Elastic vibration characteristics of cantilever plates in water. *Journal of Ship Research 9*, 11-12.

Park, J. Y. and J. E. Kim (2005). Global existence and stability for Euler-Bernoulli beam equation with memory condition at the boundary. *J. Korean Math. Soc. 42*(6), 1137-1152.

Rezazadeh, G., M. Fathalilou, R. Shabani, S. Tarverdilou and S. Talebian (2009). Dynamic characteristics and forced response of an electrostatically-actuated microbeam subjected

to fluid loading. *MicrosystTechnol 15*, 1355-1363.

Shabani, R., H. Hatami, F. G. Golzar and S. Tariverdilo (2013). Coupled vibration of a cantilever micro-beam submerged in a bounded incompressible fluid domain. *Acta Mechanica,* *Volume 224*(4), 841-850.

Wang, Y. G., W. H. Lin and N. Liu (2015). Non-linear bending and post-buckling of extensible microscale beams based on modified couple stress theory. *Applied Mathematical Modelling 39*, 117-127.